STUDIES ON GOLD NANOPARTICLE DECORATED ZINC OXIDE NANOROD-BASED LSPR SENSOR FOR THE DETECTION OF AMPICILLIN RESIDUES IN WATER

by

Khajohnpat Teerasitwaratorn

A Thesis Submitted in Partial Fulfillment of the Requirements for the Degree of Master of Science in Nanotechnology

Examination Committee: Dr. Tanujjal Bora (Chairperson)
Dr. Loc Thai Nguyen
Dr. Waleed Mohammed

Nationality: Thai
Previous Degree: Bachelor of Science in Applied Physics
King Mongkut's University of Technology
North Bangkok, Thailand

Scholarship Donor: Royal Thai Government Fellowship

Asian Institute of Technology
School of Engineering and Technology
Thailand
July 2021

AUTHOR'S DECLARATION

I, Khajohnpat Teerasitwaratorn, declare that the research work carried out for this thesis was in accordance with the regulations of the Asian Institute of Technology. The work presented in it are my own and has been generated by me as the result of my own original research, and if external sources were used, such sources have been cited. It is original and has not been submitted to any other institution to obtain another degree or qualification. This is a true copy of the thesis, including final revisions.

Date: 21st July 2021

Name: Khajohnpat Teerasitwaratorn

Signature: 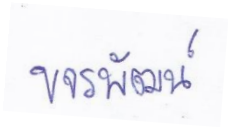

ACKNOWLEDGMENTS

First and foremost, I would like to express my sincere appreciation and gratitude to my thesis advisor, Dr. Tanujjal Bora, for offering me the encouragement, understanding, invaluable guidance, supports, and brilliant remedies for every obstacle throughout my thesis work to complete the research successfully. I have been inspired and motivated a lot by his empathy, vision, and attitude. It was very meaningful to me. I would also like to thank my thesis committee members, Dr. Loc Thai Nguyen and Dr. Waleed Mohammed, for sitting on my panel, taking the time to read and revise my thesis, and giving necessary suggestions and aspects to make this study better. It was a great opportunity and honor to study and work under their guidance. Without them, this study could not be complete and successful.

I would like to acknowledge the financial support provided to me by the RTG fellowship granted by the Thai government during my master's degree.

I am exceedingly grateful to my family for their love, caring, sacrifice, and support during my study. Nothing might be possible without them.

In addition, I am very thankful to Ms. Nutthanicha Chuanopparat, Ms. Ariya Khaowong, and Ms. Wirawee Linsuwanont for their valuable friendship, empathy, caring, and great sense of humor. Also, a big thanks to my other friends not only from the Nanotechnology program but also other programs in AIT for their constant support. Without their love and encouragement, my life during the master's degree would have been boring and exhausting.

Last but not the least, a special thank you to the 4EVE members and Ms. Suchaya Saenkhot, a member of BNK48, for their encouragement which have deeply inspired me.

ABSTRACT

The antibiotic contamination of water is one of the modern-day global concerns causing various adverse effects on humans and other living organisms. Consequently, their detection in the aquatic environment is important to ensure a healthy environment around us. In this research, we report a localized surface plasmon resonance (LSPR) based aptasensor capable of detecting trace amounts of antibiotic residues present in water. The LSPR-based aptasensor is composed of nanoscale gold (Au) particles decorated on vertically aligned zinc oxide (ZnO) nanorods where the gold nanoparticles are functionalized with aptamer specific to bind ampicillin antibiotics to the sensory surface. The study focuses on the design of the aptasensor and the effects of amounts of ZnO and Au on the sensor performance. The sensor materials are characterized with scanning electron microscopy (SEM), energy dispersive X-ray spectroscopy (EDS), and UV-Visible spectroscopy to investigate their morphology, elemental compositions, and optical properties. The developed LSPR-based aptasensor showed good sensitivity and selectivity towards ampicillin detection in water with a limit of detection close to 10 ppm concentrations of ampicillin within 20 minutes of analysis time. Results from this study showed future potential for the LSPR-based aptasensors in antibiotic detection which can offer inexpensive fabrication, high sensitivity, good selectivity, fast detection, mobility, and real-time detection.

CONTENTS

Page

LIST OF TABLES

LIST OF FIGURES

Page

LIST OF ABBREVIATIONS

ADI	= Acceptable Daily Intake
AuNPs	= Gold Nanoparticles
CDC	= Centers for Disease Control and Prevention
EOCs	= Emerging Organic Contaminants
HPLC	= High-Performance Liquid Chromatography
LOD	= Limit of Detection
LSPR	= Localized Surface Plasmon Resonance
PPCPs	= Pharmaceuticals and Personal Care Products
ppm	= Part Per Million
ppt	= Part Per Trillion
SELEX	= Systematic Evolution of Ligands by Exponential Enrichment
SPR	= Surface Plasmon Resonance
SPs	= Surface Plasmons
WTP	= Water Treatment Plant
WWTP	= Wastewater Treatment Plant
ZnONRs	= Zinc Oxide Nanorods

CHAPTER 1
INTRODUCTION

1.1 Background of the Study

Antibiotics are one type of medicines which have been widely utilized in the medical, food industry, cattle, and agriculture fields to treat bacterial infections and prevent diseases in animals, plants, and especially human. As a result, they ensure good health and increase not only the product quality but also yield sometimes. However, the residues of used pharmaceuticals may remain and possess in the products due to their improper elimination and overused in quantity and concentration. These residues can lead to food and environmental contamination posing threat to our health and ecosystem (F. Li et al., 2018a; Luo et al., 2017).

Antibiotics may enter humans, animals, and plants both directly and indirectly. The use of antibiotics in animal and agriculture may leave residues in the flesh products such as meat and eggs and environments as well, for instance, soil and water. Most of the pharmaceutical substances are polar compounds, hence, they can conveniently spread into the water source such as lakes and rivers. The consumption of antibiotic contaminated water or other food products can provide various health issues not only to humans but also animals. For example, allergy, mutagenicity, bone marrow toxicity, anaphylactic shock, and cancer (Bacanlı & Başaran, 2019; Hiep, 2020).

Currently, various methods for antibiotic residue detection are in use to evaluate the contaminated agricultural products and water due to the concern of serious environmental and health unfavorable effects from such residues. Some of these methods are colorimetric detection, Raman spectroscopy, high-performance liquid chromatography (HPLC), etc. These methods show high selectivity and sensitivity towards antibiotic residue detection. Nevertheless, they need an expensive instrumentation, complex sample preparation, and skilled operator. Furthermore, the real-time detection is not possible in most of the cases. Therefore, researchers are constantly developing new reliable and real-time methods to detect antibiotic residues and solve those problems which have been mentioned (Gai et al., 2017; F. Li et al., 2018b; Wang et al., 2016).

Optical sensors based on the surface plasmon resonance (SPR) of metal nanoparticles for chemical residue detection are obtaining significant attention in recent years due to their high detection sensitivity and simplicity to use (Homola, 2008; Masson, 2020). Surface plasmons (SPs) are coherent oscillations of free electrons at the boundaries between metal nanostructures and a dielectric medium when an electromagnetic radiation such as a light. At resonance, the oscillating SPs absorbs the radiation strongly producing a dark band in the reflected light spectrum which is the basis of the SPR sensor construction.

1.2 Statement of the Problem

SPR sensors provide a high sensitivity of detection with portability which allows these kinds of sensors to use outside the laboratory environment. However, their production cost is still high due to the use of complex optical components like prism, gratings etc. during the construction of SPR sensors. Moreover, SPR sensors utilize nanoscale thin metallic films which requires sophisticated fabrication steps. Therefore, the overall cost of the SPR detection device is increased due to the introduction of the system design complexity. A localized surface plasmon resonance (LSPR) sensor, on the other hand, has the potential to reduce the complexity in design and hence the fabrication cost of the sensors.

LSPR systems use metal nanoparticles instead of thin films and these nanoparticles can be synthesized very easily using simple wet chemical approaches. Moreover, they can be further surface functionalized for selective detection of the specific chemical and biological species. Recently, an LSPR-based sensor was successfully developed in our lab (Hiep, 2020) using gold nanoparticles (AuNPs) deposited on an array of vertically aligned zinc oxide nanorods (ZnONRs). The sensor surface was further modified with aptamers for selective detection of ampicillin residues in water. The developed LSPR sensor has a very simple design and does not require any complicated fabrication processes. The sensor was tested against three different antibiotics which were ampicillin, amoxycillin and tetracycline and demonstrated very good selectivity towards ampicillin detection in water.

However, the LSPR sensor developed in our lab has a low sensitivity at this moment and its limit of detection (LOD) is not lower enough to compete with the other SPR sensors which available in the literature. One of the major reasons for the low sensitivity

and high LOD is the small quantity of Au nanoparticles present on the surface of the ZnO nanorods. As a result, the LSPR signal received from these nanoparticles are very weak and dominated by the noise levels from the light source and the detector affecting the overall sensitivity of the detection system. Additionally, ZnO nanorods are used as a support part for the Au nanoparticle at the current design, they can affect the detection sensitivity of the sensor due to their exclusive properties as well.

ZnO is a wide bandgap metal oxide semiconductor which do not show any optical absorption in the visible region. However, due to the anisotropic nanorod shape, these nanorods can introduce scattering of light in the visible region which can interfere with the SPR signal from the Au nanoparticles. To address these issues in the LSPR sensor developed in our lab, it is therefore necessary to increase the amount of gold nanoparticles to enhance the SPR signal strength and control the amount of ZnO in the system to reduce the interference of the scattering light with the LSPR signal from the Au nanoparticles.

1.3 Objectives of the Study

The objective of this study is to fabricate an LSPR-based aptasensor using AuNPs decorated on ZnONRs and study the effects of amounts of ZnO and Au in the sensor substrate on the sensor sensitivity and LOD for the selective detection of ampicillin residue in water. The specific objectives are shown below:

1. To reduce light scattering from ZnO nanorods by controlling the length of the nanorods.

2. To increase the LSPR signal strength by controlling the amount of Au nanoparticles.

3. To fabricate the LSPR sensor for the selective detection of ampicillin in water and evaluate the sensor sensitivity and LOD.

1.4 Scope of the Study

The scope of this study is in the field of LSPR-based aptasensors for the detection of antibiotic waste residues in water. The LSPR sensor developed in this research utilizes ZnO nanorods as a support component and gold nanoparticles as the visible light active

LSPR component to provide detection. An aptamer is used to functionalize the surface of AuNPs to improve its selectivity towards ampicillin.

1.5 Organized of the Report

This report is divided into five chapters which are included as follows: *Chapter 1* described the background, statement of the problems, objectives, and scope of the study. *Chapter 2* discusses the relevant literature including general information related to the subject of the study and the finding of previous research. *Chapter 3* provides the description of the research methodology used in this study. *Chapter 4* presents the experimental results of the study and discuss them. *Chapter 5* summarizes the research work performed. It develops a clear view about the study in the form of conclusions and future recommendations.

CHAPTER 2
LITERATURE REVIEW

2.1 Pharmaceutical Residues in the Environment

Pharmaceutical wastes are wastes generated from unused, expired, contaminated, damaged, or improper disposed medicines. The pharmaceutical wastes or residues in the environment is on a continuous rise due to its wide uses in households, hospitals, and cattle farms. However, these residues possess adverse effects on human health and the ecosystem. If entered into human body, these wastes can cause diseases which are difficult to treat. Antibiotic residues in ecosystem can produce resistance in bacteria against antibiotics creating a complex bacteria class known as *antibacterial-resistant-bacteria* (ARB). ARBs are capable of causing serious disease and become resistant to most commonly available antibiotics. They are becoming a serious public health problem. In this section we give a brief overview on various pharmaceutical residues found in environment, their sources and adverse effects on living organisms.

2.1.1 Antibiotic Residues in the Environment

There are various types of emerging organic contaminants (EOCs) compounds occurred in the groundwater such as pharmaceuticals and personal care products (PPCPs), pesticides and industrial compounds from the food production and preservation (Lapworth et al., 2012).

Pharmaceuticals are the synthetic organic substance which are fabricated to use in a variety of purposes. They are typically used not only for therapeutic purposes such as treating and preventing the deadly infections in patients, plants, and livestock but also nontherapeutic aims like growth promotor in food animals (Gelband et al., 2015).

The pharmaceuticals are classified by their chemical structure and usability into six common types which are an analgesic, antibiotics, cardiovascular pharmaceutical, psychostimulants, hormonal compounds, and antiepileptic drug. The drugs in the same class possess a homologous structure, active mechanism, aim of use, and behavior to the environment (Huang et al., 2001). The different aims of use are represented for each type of the pharmaceutical due to their contract in activity with the consumer body and nerve system (Li, 2014; Hiep, 2020). For instance, an analgesic or typically known as

a pain killer is a drug used to mitigate or alleviate the pain represented from diseases by acting in the diverse strategies on the central nervous systems and their peripheral of the consumers (Bueno et al., 2012; W. C. Li, 2014) and an antibiotic which is one kind of pharmaceutical where is able to kill and break the growth of bacteria. They might be created naturally by living things or synthesized in laboratory circumstance. Antibiotics have been commonly used in medicine as antimicrobial drugs for disease treatments for humans, animals, and plants (Bacanlı & Başaran, 2019a).

There are more than 3,000 pharmaceutical components which are produced, commercialized, and used in the medical and industrial fields at present (Hiep, 2020).

Antibiotics are the common pharmaceutical which can be utilized in a hospital, medical center, agriculture, ranch, and human community. Some recent studies indicate that more than 63,200 tons of antibiotics were used in food animals, this number is more than the amount of use in all human and tends to increase continuously in every year (Gelband et al., 2015). Consequently, due to a rising of the demand for antibiotics around the world and their uses, significant amount of these drugs is leaking to the environment where antibiotic residues have been now found in ecosystems, some of which are soil and water sources.

2.1.2 Sources of Antibiotic Residues

Pharmaceuticals and other EOCs compounds can wade the environment by a lot of sources and pathways and the major source of the EOCs in the ecosystem is the waste-water (Lapworth et al., 2012).

The sources of EOCs can be divided into two types: point source and non-point or diffuse source. The point source contamination generates from a specific source which can be defined as a location such as a residue from manufacturing plants, hospital, and domestic. Point source pollution typically presents in large loading to a specific area, and it can cause the facile monitoring in the ecosystem. The highest median of the EOCs according to the landfill sources. On the other hand, the non-point source or diffuse contaminations can be defined as the residues that are created from broad area of source and the specific location of the source cannot be defined such as the antibiotic waste from farm and household. The residue loading from the diffuse source often lower than

point source. Mostly of antimicrobial residues come from the non-point source due to the covering in large scale of source (Hiep, 2020; Lapworth et al., 2012).

Antibiotics typically use with the therapeutic purpose to cure the fatal diseases in human, animals, and plants. In currently, better living circumstances provided from the prosperity in every country result in the increasing in pharmaceutical requirement. For instance, the elongation of human life expectancy leads to the existence of the aging society, it might result in enhancement of the PPCPs requirement for patients and elderly people in hospital or medical centers (W. C. Li, 2014). Additionally, the fleet population, and economic growth around the world lead to the more need of an animal protein and agricultural products cause the nontherapeutic use of the antibiotic as the growth promotor in food production to overcome the growth limitation of food animals and plants (Bacanlı & Başaran, 2019b; Gelband et al., 2015).

The pharmaceutical wastes are defined as expired drugs, contaminated products, and unwanted dispensed medicines (Kadam et al., 2016). Most of the antibiotic residues in the environment are demonstrated from the non-point source. In most countries, around 20 percent of pharmaceutical are used in the healthcare center and hospital, while approximately 80 percent are used in the community.

Common drugs are purchased directly by a consumer from the pharmacy or provider without the prescription from doctors or specialists. It results in the improper use and elimination of drugs which can lead to the occurrence and discharge of the antibiotic residue in human and environment. For example, in China, where a medical prescription is do not needed for medicine purchasing, antibiotics are extensively used with high amount resulting in the high concentrations of the antibiotic residue in the environment (Gelband et al., 2015; W. C. Li, 2014).

The pharmaceutical waste can enter aquatic environment from various of fountainhead and pathways. There are five essential sources of the pharmaceutical residue discharge which are veterinary, domestic, hospital, industrial, and landfill waste and domestic households are one of the most common sources for these wastes reaching to our environment as showing in the Figure 2.1 (Bound & Voulvoulis, 2005; W. C. Li, 2014).

In accordance with the legislation, the unwanted drugs will be buried or incinerated at the specific landfill sites accommodated for the toxic waste to eliminate the unwanted

drugs. However, the residues might be disposed to the soil and water sources in the end. Even though the manufacture who fabricate the pharmaceuticals always recommends the consumer to return the expired or unwanted drugs to them even the drug disposal is expensive than manufacturing cost, the waste disposal via sink/toilet still common in the society due to the simple and lack of the control (Bound & Voulvoulis, 2005; Kadam et al., 2016). Therefore, the several literature reported that the pharmaceutical waste detected in the water source represents the higher concentration than soil (Bound & Voulvoulis, 2005; Lapworth et al., 2012; W. C. Li, 2014).

Figure 2.1

The Possible Sources and Pathways of Pharmaceutical Entering Aquatic Environment

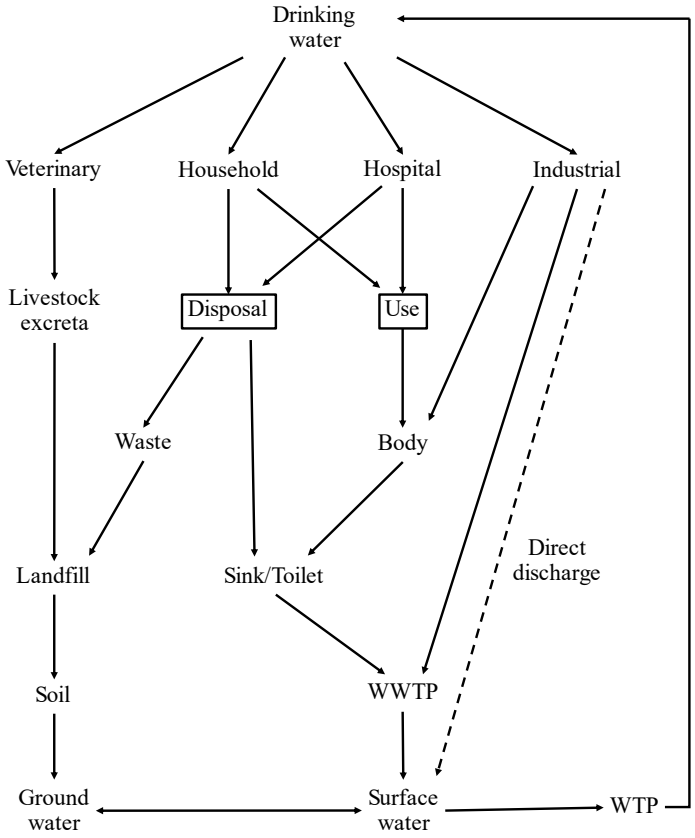

Note. Adapted from "Household disposal of pharmaceuticals as a pathway for aquatic *contamination in the United Kingdom" by Bound, J. P., & Voulvoulis, N., 2005, Environmental Health Perspectives, 113(12), 1705–1711. (https://doi.org/10.1289/ehp.8315), and "Design and fabrication of microfluidic LSPR sensor for antibiotics waste detection" by Hiep,L.T., 2020, AIT Master Thesis.*

One of the major causes of the drug residue in the wastewater is the uncompleted metabolism of the consumer not only human, but also animals. Only the active ingredient of the medicine can be metabolized, and the rest of non-metabolized compound was discharged to the water source. Also, the incomplete remove of the waste from the wastewater treatment plant (WWTP) and water treatment plant (WTP) due to the ineffective in the treatment (Huang et al., 2001; Kadam et al., 2016; W. C. Li, 2014; Vieno et al., 2007).

The average efficiency for the sewage treatment is varied from 20% to 99% depends on the substances and the range of the untreated sewage water with the antibiotic residue is from 3.9 ng/L to about 27,000 ng/L (Bueno et al., 2012; Huang et al., 2001).

2.1.3 Effects of Antibiotic Residues in Living Organisms

The antibiotics is invented to treat bacterial infections and expand the growth efficiency by having an action against the nerve system and other organs (Franco et al., 1990; W. C. Li, 2014). Even though the pharmaceutical residues in aquatic environment are attenuate by the physical and biological processes, the amount of the drug waste in soil and water still high and can affect the consumers who take these residues intentional and unintentional because the medicines are designed to active with the target at a low concentration. Therefore, the pharmaceutical pollutants even in the lower amount than part per trillion (ppt) in the environment might surpass an acceptable daily intake (ADI) and provide an activity to the consumer lead to the adverse effects (Hammesfahr et al., 2011; Kadam et al., 2016; Murray et al., 2010).

There are three serious effects of antibiotic residues on living things which are particularly concerned. Firstly, the pharmaceutical allergic on people who consumed. The allergy effects might be proposed to the consumer who accidentally take the antibiotic residue even though small amounts. There are a number of studies reported that the allergic reaction result in the antimicrobial intake in human and the misery of the symptom depends on the amount of residue intake and consumer's body. However, the most serious effect is death (Bacanlı & Başaran, 2019a). Additionally, it can cause the acute failure in organs due to the overtimed drug residue elimination in the body.

Secondly, the incoming of the antibiotic resistance not only in people and animals, but also the bacteria. The high amount and improper use of drug for fever and coughs with

erroneous drug cannot treat the pathogen, but it increases the load of the antibiotic-resistant infections in the consumer. The U.S. Centers for Disease Control and Prevention (CDC) forecasts that in United States, around not only 2 million infections, but also 23,000 deaths each year plus about 25,000 deaths in Europe occur due to the consumer's antibiotic resistance. Antibiotics using can decrease the drug effectiveness and increase the consumer's drug resistant. Consequently, antibiotics should be utilized only when they are needed to lower the drug resistant issue (Gelband et al., 2015; Lee, M.H., Lee, H.J., Ryu, 2001; W. C. Li, 2014; Marshall & Levy, 2011). Finally, according to the drug resistant, the occurrence of pharmaceutical contamination in the environment and biological organisms can affect soil microbial biomass, aquatic ecosystem, and global in bad ways. For instance, the algae in antibiotic contaminant aquatic environment might possess the effect on the chloroplasts which are the major basis of the photosynthesis results in the unfavorable effect to the water source and ambient (Bound & Voulvoulis, 2005; Hammesfahr et al., 2011; Hou et al., 2015; W. C. Li, 2014).

2.1.4 Ampicillin

Ampicillin drug is one kind of antibiotics which widely used in human medicine (Marshall & Levy, 2011). Ampicillin belongs to β-lactam/ β-lactamase class produced for the incoming of resistant bacterial mutants. It is typically utilized to treat the bacterial infection such as gonorrhea, venereal diseases and the infections of ear, lungs, and nose due to the reaction against bacteria with Gram-positive and Gram-negative types. Ampicillin is widely used in the present due to the broad spectrum of treatment, low cost, and various alternate form of use (Rafailidis et al., 2007; Shrivas et al., 2017). Ampicillin interrupts the synthesis of bacterial cell wall by attaching to the specific enzyme liable for the cell wall formation which called penicillin binding proteins (PBPs). However, the large amount of ampicillin reaction can cause its prevention from hydrolysis by β-lactam. As a result, from the tolerance of the ampicillin, adverse side effects can be occurred such as dizziness, skin rashes, and pain at the injection intramuscular. In addition, a stomach cramps and diarrhea can be provided due to the intestinal bacteria inhibiting needed for food digestion in body (Rafailidis et al., 2007; Shrivas et al., 2017).

2.2 SPR/LSPR Sensors for Antibiotic Residue Detection

Optical and electrochemical properties are generally considered to design and fabricate the sensors. Nanomaterial provides different optical, chemical, mechanical, and electronic features compared to bulk materials and these differences can be applied in various ways to generate superb technologies in many fields of study. Most of optical sensors use the plasmonics, Raman, UV-visible light, and fluorescence to detect and evaluate the analytes. There is one interesting optical phenomenon generated by electromagnetic wave when it associates with the conductive nanoparticles called surface plasmon. This phenomenon has attracted the interest of the scientists due to its broad spectrum of use. Therefore, the sensor based on surface plasmon method relied on the changes of the refractive index emerging from the caged of the metal particles on the plasmonic surface has been studied and developed in the past many years for a number of purposes and applications such as the clinical diagnostics, tiny particle sensing, and food monitoring. (Hiep, 2020; Masson, 2020).

Figure 2.2

Principle of SPR

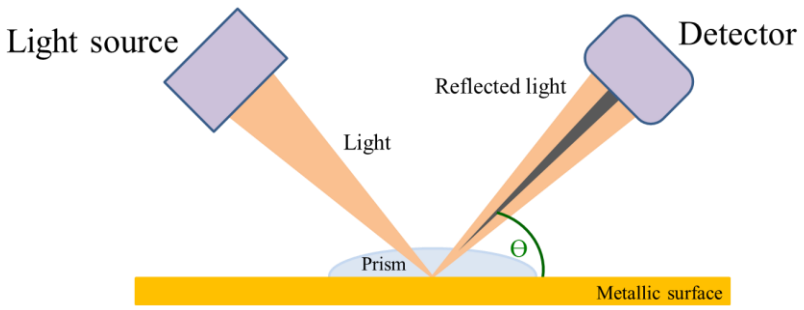

Surface plasmon resonance (SPR) is an optical phenomenon utilized as a transducer in various chemical and biosensors. It is considered as a phenomenon occurred when the oscillated electron at the thin layer noble metal surface is resonant with propagating electromagnetic wave at the metal-dielectric interface (Cao et al., 2011). The oscillation of electrons arises at the boundary between dielectric material and plasmonic surface. The total energy of surface plasmon is a function of the dielectric constant of the plasmonic material and light wavevector (Masson, 2020). A diagram showing a basic principle of SPR is represented below.

The light from the light source is irradiated through the field of electrons called prism and reflects off the surface. Then, the reflected light with the dark band at a certain angle is collected by the light detector. This dark band results from the reflected light intensity loss due to the light absorption of the electrons at the metallic surface (resonance wavelength). Absorbed light is used to generate the resonance of the electrons and these resonating electrons are called surface plasmon resonance. The angle of the light absorbed by the plasmonic surface is changed related to the changes in the refractive index and the dielectric constant near the surface boundary.

SPR is utilized to identify a quantity of targeted molecules by analyzing resonance angle shifts from the changes in the refractive index of prism when the undefined molecules in the bind with the probe molecules at the sensing surface (SPRtech101, 2011; Hiep, 2020)

Localized surface plasmon resonance (LSPR) is related to SPR, usually created by noble metal nanoparticles. It is a widespread practical approach for the various substance analysis and thereby has attracted attention of numerous researchers around the world due to its advantages such as the simplicity, rapidly, accuracy, and reliable. Additionally, the high sensitivity LSPR sensor for any chemical detection can be provided due to the nanomaterial use in the sensor (Masson, 2020).

Figure 2.3

Plasmon Oscillation of Spherical Metal Nanoparticles

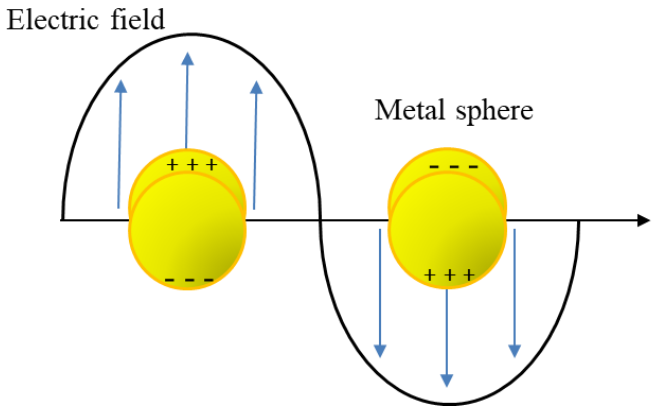

The major difference between SPR and LSPR is the length of the plasmonic material confinement. In SPR, the thin metallic film possesses a large dimension than the wavelength of the incident light result in the propagation resonance of the plasmon on

the plasmonic film while the LSPR plasmonic materials possess the smaller size than the wavelength of the incident light causes the confined electron oscillation at the plasmonic surface. The ratio of the light scattering and absorption alter related to the size of metal nanoparticles. The large particles offer the very high light scattering opposite with the high absorption in the small nanoparticles (Sönnichsen, 2001)

LSPR is produced when the interaction of light and conductive particles which have a smaller dimension than the wavelength of light is offered. The conductive nanoparticles and their surface electrons started an oscillation when they are excited by an optical beam. Electric field is formed due to the confined oscillations of the surface electrons of the position restricted conductive atoms which occur to fix the charges of the system (Masson, 2020; Petryayeva & Krull, 2011; Smith, 2007; Srivastava et al., 2012).

The frequency of the electron oscillation is imposed by various factors such as the size, shape, composition, and polarizability of the conductive nanoparticles, including the surrounding medium and the coherent localized oscillation of the plasmon at a resonant frequency is created when the frequency of incident light is resonant with the electron oscillations of the conductive nanoparticles (Cao et al., 2011; Petryayeva & Krull, 2011; Srivastava et al., 2012).

According to the localized of the metal nanoparticles, the particles can reach the maximum optical absorption plasmon frequency. The frequency of plasmon resonance is very sensitive to the refractive index of the ambient cause the shift in the resonance frequency. The easy in measurement of resonance frequency allow the LSPR sensor to evaluate the nanoscale sensing (The Audiopedia, 2018)

At the resonance frequency of the exciting field and an oscillation of electrons, changes in the surrounded refractive index around the nanoparticles can be provided, which lead to the modify of optical properties of nanoparticles such as light absorption and scattering and thereby a high sensitivity of LSPR sensor can be promoted (Petryayeva and Krull ,2011; Srivastava2012; Masson, 2020).

The mechanism of LSPR can be explained like when the electromagnetic wave such as light is irradiated to the plasmonic surface, the free electrons on the surface are exited and provided the movement of the electrons. The particle polarization also occurred due to the light irradiation.

When the light with the larger wavelength than the metal nanoparticles go through the molecules, the metal nanoparticles are absorbed or induced by the light and start oscillation causes separation of negative charge and positive charge region. The oscillation of the surface electrons is called “plasmon”. The enhancement of the plasmon field due to the oscillation on the plasmonic surface causes the change in the refractive index and the resonance frequency is changed (Hiep, 2020).

LSPR approach is the extensively and frequently method used in the substance analysis because of their significant benefits. For example, small sample volume and small sensory surface are required, sensitivity of LSPR sensor can be optimized by controlling the changes in sizes, shapes, and components of the nanoparticles, the instrument required for LSPR is simple, easy to use and maintain due to no strict of temperature control, no need of prism and reflected angle for analysis. Furthermore, a high sensitivity to small refractive index changes is offered causes of a short decay length of relative electromagnetic (EM) field (Cao, 2011; Nicoya Lifesciences, 2016; “LSPR vs. SPR”, n.d.). Even though LSPR sensors provide excellent sensitivity and selectivity of specimen detection, the identification of the petite concentration of the sample such as insecticide or antibiotic waste residue may not be afforded. Consequently, LSPR sensors are usually used beside some exclusive complements or techniques to improve their detection efficiency and increase their limit of detection (LOD) to reach the substance analysis with the small concentration of targeted molecules.

2.2.1 Localized Surface Plasmon Resonance Sensors

Localized surface plasmon resonance sensors applied LSPR phenomenon for various purposes such as insecticide residue detection on the agricultural products, and the detonation compound analysis. Also, the detection of the antibiotic residue in the environment with a little magnitude (Petryayeva and Krull ,2011).

LSPR sensors can be used to identify substances by analyzing changes in specific properties of LSPR component before and after interacting with the sample. A colorimetry is the most attractive analytical technique for sample examination. It diagnoses the substances by detect or measure changes of their optical signal which is a change of color or a shift of light absorption peak and LSPR signal. LSPR colorimetric sensors recently widely use for the chemical detection due to their various advantages such as the simplicity, low cost, reliable, and rapidly detection (Feng et al., 2018;

Rostami et al., 2020). Several instances of the colorimetric sensory devices utilized LSPR method are represented below.

Table 2.1

Examples of LSPR Sensors Used for Chemical Detection

Application	Nanostructure	Detection limit	Reference
Glucose concentration determination	Gold nanorods	18 ppm	(Lin et al., 2016)
Ampicillin detection in human urine	Silver nanoparticles	0.01 ppm	(Shrivas et al., 2017)
Detection of Pb^{2+} ions	Indium tin oxide / glutathione / gold nanoparticles	0.01 ppm	(Feng et al., 2018)

2.3 Aptamers in Pharmaceutical Residue Detection

SPR and LSPR sensors have shown promise for sensitive chemical detection even at extremely low concentrations. However, most of the time they fail to selectively detect target chemicals in complex real samples. As a result, they lose their practical usability. Additional sensor surface modification is typically done to avoid such issues and make these sensors selective. Amongst various surface modification techniques, functionalization of the metal nanoparticle's surface with aptamers is an interesting approach to achieve high selectivity.

Aptamers are synthetic ligands generally made up of single-stranded oligonucleotides that can selectively bind to a specific target, including proteins, peptides, carbohydrates, small molecules, toxins, and even live cells. They, therefore, offer high affinity and specificity towards binding to a specific targeted molecule, like (O'Sullivan, 2002; Tombelli et al., 2005).

Aptamers are accepted by the national as a superior to antibodies due to their several advantages. For example, the very high selectivity and affinity to their target molecules are offered because aptamers are synthetic nucleic acids then either shape of the

aptamers and oligonucleotide sequences can be designed by the producer. Therefore, selectivity, affinity, and several properties of aptamers may better than antibodies. Aptamers can be generated by an in vitro method which can overcome the limitation of physiological recognition of the in vivo method. Also, the in vitro synthetic method can reduce a time for in vivo detection from weeks or months to only a few days (Cho et al., 2009; O'Sullivan, 2002; Tombelli et al., 2005).

The molecule selection by an in vitro process is called systematic evolution of ligands by exponential enrichment (SELEX). The SELEX method offers a unique oligonucleotide target molecules identification from various oligomers with the random sequence. A variety of molecules are put to the SELEX process which the several of them that fit to the aptamer units can be isolated and others will be removed. Then, the fit-binding molecules will be used in the analysis (Cho et al., 2009; Lim et al., 2010; O'Sullivan, 2002; Tombelli et al., 2005).

Consequently, the aptamers can be applied to any sensors include the LSPR sensors as a receptor part to improve the sensitivity and selectivity of the sensors by utilizing the properties of aptamer. These kinds of sensor which composed of aptamer are coined aptasensors.

Lee, 2018 invented an optical fiber-based LSPR aptasensor used for quantitative detection of Ochratoxin A (OTA) composing OTA aptamer modified gold nanorods decorated on the core of optical fiber functionalized by thiol on surface. The detection of OTA is tested by dipping this LSPR aptasensor to the solution, after the sensor is removed from the sample, LSPR extinction spectral is recorded and analyzed. The result represents that a linear response is offered by the LSPR signal peak shift information and the OTA concentration detection limit is 12.0pM. In addition, high selectivity for OTA against mycotoxins such as zearalenone (ZEN) and ochratoxin B (OTB) is provided.

Besides, Li, 2018 reports the electrochemical aptasensor which developed for the multiple antibiotics utilized metal ions as signal tracers and nanocomposites as signal amplification. Metal ions such as Cd^{2+} and Pb^{2+} are mixed with the kanamycin aptamer (KAP) and streptomycin aptamer (STP) to make aptamers labels. These aptamer solutions are used to functionalization the sensing surface to increase the efficiency of

targeted molecule attachment. The kanamycin (KAN) and streptomycin (STR) concentrations are measured by differential pulse voltammetry (DPV) method and the signal strength of the system modified aptamer is about 4.6 times compared with the system without aptamer.

CHAPTER 3
METHODOLOGY

3.1 Research Framework

3.1.1 To Reduce the LSPR Signal Interference with Light Scattering from ZnO Nanorods

Inputs	Processes	Outputs

• Glass substrate
• Zinc acetate
• Ethanol
• Zinc nitrate
• Hexamine
• DI water
• Temperature
• Microwave radiation
	• ZnO nanorods fabrication from ZnO nano seeds
	• Optimization of the amount of Zn substrate concentration and volume
	• Characterizations of fabricated nanocomposites
	  ○ UV/Visible spectroscopy
	  ○ FE-SEM
		• ZnO nanorods cated glass support substrate for the LSPR sensor
		• Light absorption spectra of synthesized substrate
		• Morphology of ZnO nanorods

3.1.2 To Increase the Strength of LSPR Signal by Controlling an Amount of Au Nanoparticles

Inputs	Processes	Outputs

• ZnO nanorods substrate
• Gold chloride
• Ethanol
• DI Water
• UV radiation
• Temperature
	• Au nanoparticles decorated on ZnO nanorods surface
	  ○ Optimization of the amount Au nanoparticles by varying the number of deposition cycles
	• Characterizations of fabricated nanocomposites
	  ○ UV/Visible spectroscopy
	  ○ FE-SEM
	  ○ EDS
		• LSPR sensing surface containing Au nanoparticles on ZnO nanorods
		• Light absorption spectra of Au-ZnO substrate
		• Morphology of ZnO nanorods with Au

3.1.3 A Functionalization of Ampicillin Aptamer (AMP17) on Fabricated LSPR-Sensing Surface for Sensitivity and Selectivity Enhancement

Inputs	Processes	Outputs
• AMP 17 • Tris-HCl buffer • EDTA buffer • DI water	• AMP 17 functionalization on fabricated LSPR sensor by incubation and self-assembly approach • Characterizations of fabricated nanocomposites ○ UV/Visible spectroscopy	• Aptasensor for the detection of ampicillin in water • Sensor characteristics

3.2 LSPR Substrate Fabrication

3.2.1 ZnO Nanorods Synthesis

Hydrothermal growth method was used to synthesize ZnO nanorods on glass substrates First, glass substrates were thoroughly cleaned by dish detergent to remove any oil stains and fingerprints. Then, they were sonicated in an ultrasonic bath with acetone, ethanol, and deionized (DI) water for five minutes with each chemical. Cleaned glass substrates were dried at 90 °C for 30 minutes and stored for further use.

Figure 3.1

ZnO Nano Seeding by Spray Coating Process

Afterward, a ZnO nano seed thin layer were deposited on the cleaned glass substrates by spray coating approach. 1 mM of zinc acetate solution in ethanol was sprayed on the surface of the glass substrates kept 60 °C on a hot plate, as shown in Figure 3.1. Then, coated samples were annealed at 250 °C for five hours to allow the formation of ZnO nano seed layer on the glass substrate.

To grow ZnO nanorods, ZnO nano-seeded samples were placed in an aqueous solution of equimolar zinc nitrate and hexamine by using thin glass pieces as bases to lift the workpieces up a little bit to allow the flowing of the growth solution in and out. Also, the seeded samples were placed on the bases with the face down arrangement to allow the vertical growing of the ZnO nanorods. The concentration of zinc nitrate and hexamine were varied from 1 mM to 5 mM to control the magnitude of fabricated ZnO nanorods.

Figure 3.2

Experimental Setup for ZnO Nanorod Hydrothermal Growth

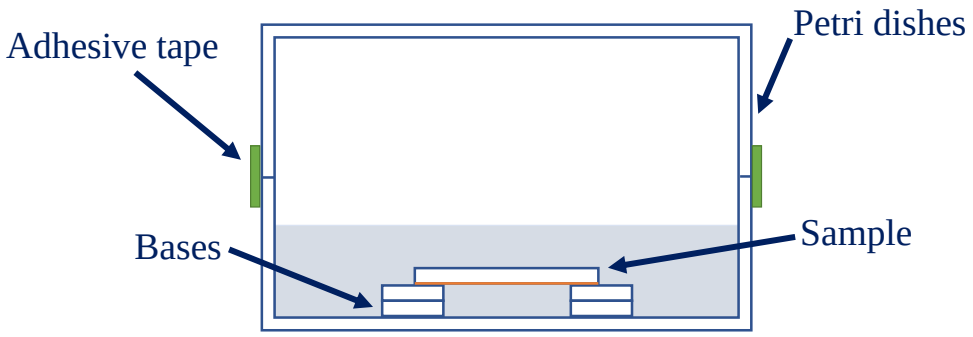

Samples was irradiated with microwave radiation for 30 minutes in the chamber which composed of two articulated medium petri dishes sealed their seam with adhesive tape (as shown in Figure 3.2) to control two significant factors of the synthesis by hydrothermal approach which are the temperature and pressure inside container. Then, after the microwave irradiation was finished, the samples were placed further inside the container for 10 minutes without irradiation for the cooling down before taken out and cleaned with DI water for several times. The nanorod growth was repeated with the varied number of cycles from 1 to 6 for each concentration to obtain the ZnO nanorods with different dimension. When the last cycle of nanorod growth had finished, irradiated samples were cleaned with DI water again before the annealing at 350 °C for

one hour. Eventually, after the samples were cooled down, glass substrates with a different thickness of ZnO nanorods layer on the surface were obtained. The samples with the ZnO nanorods on the surface were then kept in a desiccator for further use.

3.2.2 Au Nanoparticles Decoration on Aligned ZnO Nanorods

A photoreduction method followed by a heat annealing was used to decorate Au nanoparticles on fabricated ZnO nanorods. Firstly, 0.2 mM gold chloride solution in 10 mL was prepared from the dilution with 50% ethanol and 50% DI water from 10 mM $HAuCl_4$ aqueous stock solution.

Then, fabricated ZnO nanorods substrate was dipped into 10 mL of prepared gold chloride solution and irradiated with 370 nm UV light. The sample was removed from the gold solution after 5 minutes and cleaned with DI water for several times. The gold deposition process was repeated with varied number of cycles from 2 to 6 cycles to vary the amount of Au nanoparticles on the ZnO nanorod substrate. The Au decorated samples were finally annealed at 450 °C for one hour and the finished samples were then stored in a dry cabinet to prevent the air and moisture from the ambient.

3.3 Sample Characterization

The ZnONRs and AuNPs decorated ZnONRs samples were then characterized to investigate their morphology, element composition, and optical properties, Table 3.1 lists the various techniques used to characterize the samples.

Table 3.1

Techniques Used for Sample Characterization

Techniques	Evaluated factors	Model
Energy Dispersive X-ray Spectroscopy (EDS)	Elemental analysis	Oxford X-Max 20, UK with INCA software
Field Emission Scanning Electron Microscope (FE-SEM)	ZnO and Au/ZnO substrates' morphology	JEOL JSM7800F, Japan with PCSEM software
UV/VIS Spectroscopy	Optical absorption of the materials and LSPR sensor	Ocean optics USB4000 with spectrasuite software

3.4 Functionalization of AMP17 Aptamer on the Fabricated LSPR Sensing Surface

3.4.1 AMP17 Aptamer Preparation

The optimized concentration and incubation time of aptamer were used on the LSPR sensing surface functionalization to obtain the highest performance of the sensors.

A 500 mL of Tris-EDTA (TE) buffer with pH = 8.0 ± 0.01 was prepared by mixing 5 mL of 1 M Tris-Cl (pH = 8.0) with 1 mL of 0.5 M EDTA (pH = 8.0) follow by adding 494.0 mL DI water to achieve the final volume of 500 mL. The TE buffer was gently mixed and stored at room temperature.

Figure 3.3

TE Buffer pH Measurement via pH Meter

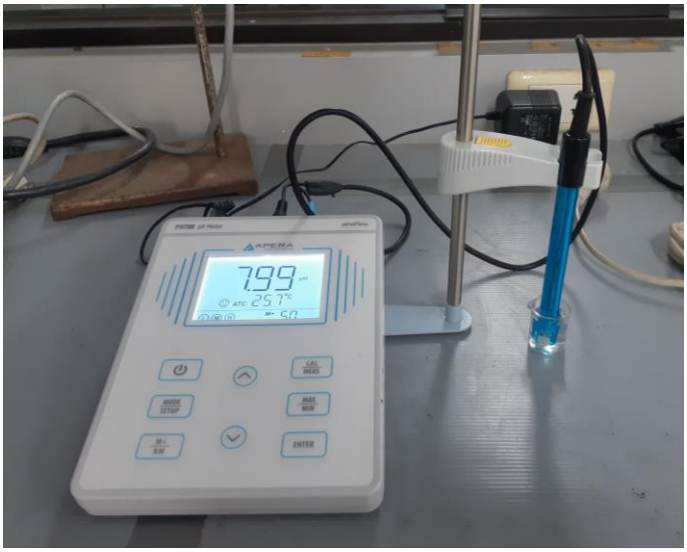

A stock solution of 100 µM AMP17 was prepared by adding 218 µL of TE buffer then centrifuged by a microcentrifuge machine at 4,000 rpm speed for 60 seconds. Activated aptamer tube was neatly covered with an aluminum foil to avoid the sunlight and stored in -20 °C non-defrosting freezer. The diluted AMP17 aptamer solutions with 1 µM concentration was used to functionalize on LSPR sensing surface and analyze its performance in the ampicillin detection.

3.4.2 AMP17 Coating on LSPR Sensing Surface

100 µM aptamer stock solution was diluted to 1 µM concentration by using TE buffer as the soluble. 225 µL of the diluted 1µM AMP17 solution was put to the Eppendorf tube then the LSPR surface consisting of ZnO nanorods decorated with Au nanoparticles were incubated in the aptamer solution for 30 minutes to allow the formation of aptamer-LSPR sensing surface by the self-assembly approach. The functionalized sample was cleaned with TE buffer for several times after removed from the incubation container.

The optical absorption spectrum of the same LSPR-based sensing surface before and after aptamer functionalization on the surface were measured by using the UV/Visible spectrometer and then the LSPR peak shift information was offered afterward.

Figure 3.4

LSPR Surface Functionalization with AMP17

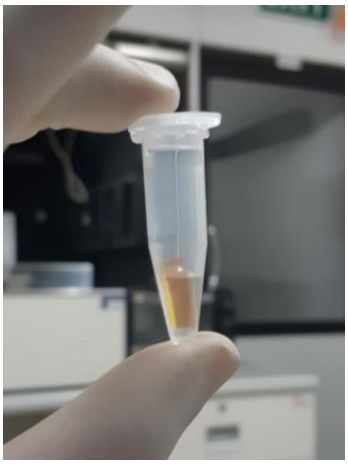

3.5 Sensitivity Testing of AMP17 Aptamer-LSPR Sensor

The sensitivity of aptamer-LSPR sensor was assessed with the detection of DI water included with several concentrations of ampicillin. After the sensing surface was functionalized its surface with AMP 17 and the apta-LSPR sensor was obtained, the fabricated sensor was incubated in the diluted ampicillin aqueous solution with different concentrations (10 ppm, 1 ppm, 0.5 ppm, 0.1 ppm, and 0 ppm or blank sample) for 10 minutes. After that, the sensor was removed from the solution and placed in the room temperature until dry before collected the light absorption and indicated the LSPR peak shift by comparing the peak positions of Au nanoparticles before and after ampicillin

measurement. Subsequently, the LSPR peak shift was calculated and the limit of detection (LOD) and sensitivity of the fabricated sensor was evaluated from the blank determination with the equation 3.1 (Anumolu, 2014; AS, 2021).

$$LOD = 3.3 \times \frac{SD}{S} \tag{3.1}$$

Where, *SD* is the standard deviation of the blank sample and *S* is the slope obtained from the linear regression line (Shrivastava & Gupta, 2011).

CHAPTER 4
RESULTS and DISCUSSION

4.1 ZnO Nanorods Growth and Characterization

4.1.1 Morphological of the ZnONRs

ZnO nanorods were synthesized hydrothermally on glass substrates and characterized by using scanning electron microscope (SEM) to investigate their morphology. Figure 4.1 shows the SEM micrographs of ZnO nanorods grown on glass substrates using two different growth solution concentrations, viz. 3 mM and 5 mM and the growth cycles were varied as 4 and 6. From the SEM images we can see the characteristics hexagonal shape of the ZnO nanorods standing almost perpendicular to the surface of the glass substrate.

Figure 4.1

SEM Micrograph of Hydrothermally Growth ZnO Nanorods.

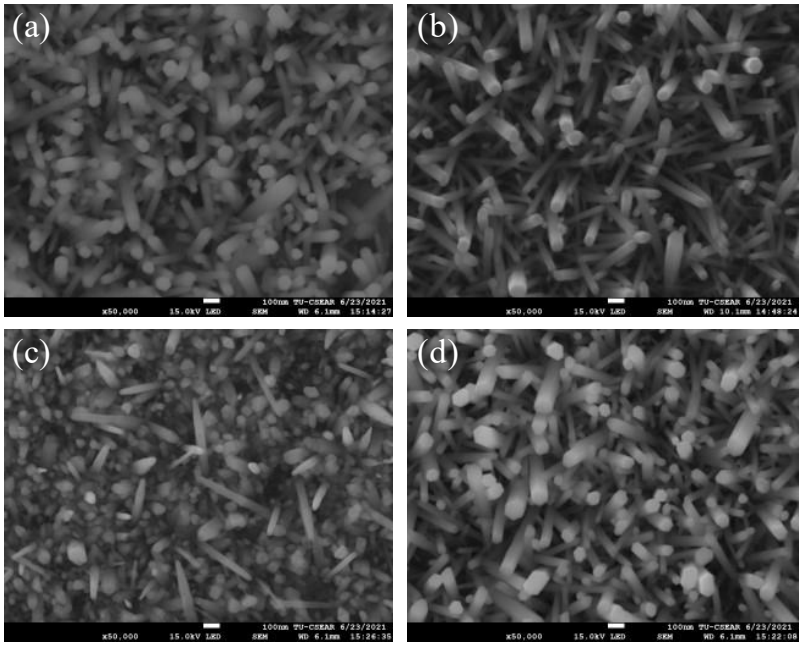

Note. The ZnO nanorods were grown hydrothermally on glass substrates using two different growth solution concentrations and at two different numbers of growth cycles. (a) 3 mM - 4 cycle, (b) 3 mM - 6 cycle, (c) 5 mM - 4 cycle, and (d) 5 mM - 6 cycle, respectively.

From the SEM images, as shown in Figure 4.1, it was also observed that the overall number of nanorods per unit area or the coverage factor of the nanorods slightly decreased in both the concentrations when the number of growth cycles was increased from 4 to 6. Additionally, the 6 cycle samples also exhibited nanorods with larger diameters compared to the 4 cycle samples. The decrease in the coverage factor of the nanorods and their increased diameter at higher growth cycles can be attributed to the Ostwald ripening effect where smaller nanorods aggregate to form larger in diameter and longer nanorods reducing the overall coverage factor.

Figure 4.2

Average Diameter of the ZnO Nanorods Synthesized with Different Number of Growth Cycles.

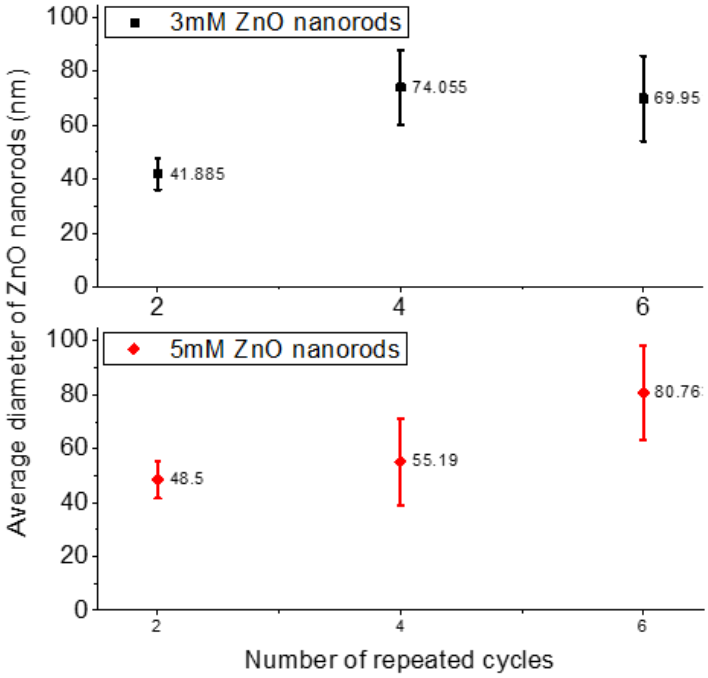

The average diameter of the nanorods, as shown in Figure 4.2, indicated gradual increase with the increasing growth cycles. For the 3 mM samples, the average diameter of the ZnO nanorods increased from ~40 nm at two growth cycles to ~70 nm at six growth cycles. Similar trend was observed for the 5 mM samples where the average diameter of the ZnO nanorods increased from ~48 nm to ~80 nm when the number of growth cycles was increased from 2 to 6, respectively.

4.1.2 Optical Absorption of the ZnONRs

The UV-Visible spectroscopy was used to collect and study the optical absorption characteristic of the ZnO nanorods. Figure 4.3 provides the information about the light absorption spectra of the ZnO nanorods where the concentration of growth solution and number of growth cycles for synthesis were varied from 1mM to 5mM and 1 to 6 cycles, respectively. As it can be seen in Figure 4.3, the optical absorption of ZnO nanorods possessed a prominent absorption in the UV range and fall sharply after around 370 nm with a very low light absorption in the visible region.

Figure 4.3

Optical Absorption Spectra of ZnO Nanorods

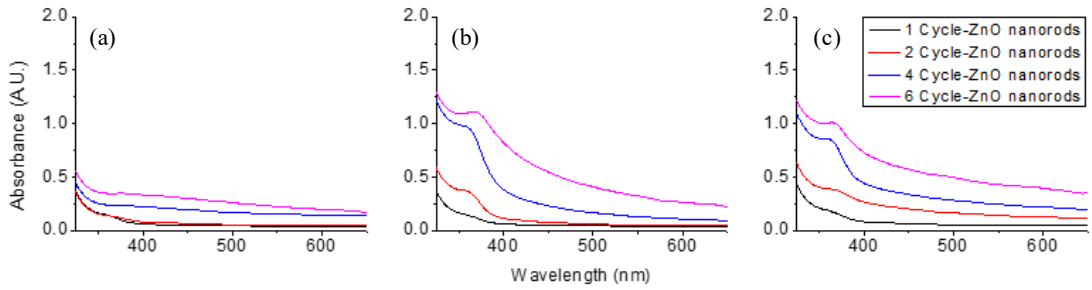

Note. (a), (b), and (c) are the light absorption spectrum of ZnO nanorods made from 1mM, 3mM, and 5mM of growth solutions, respectively.

Optical absorption of the ZnO nanorods synthesized with the same growth solution concentration with increasing number of repeated cycles was observed to increase in the UV region. At 1mM growth solution concentration (mentioned as 1mM ZnO nanorods here after) represented the lowest light absorbance compared to the ZnO nanorods fabricated with other concentrations of growth solution. However, at 1 mM concentrations the optical absorption spectra of the ZnO nanorods was found very low indicating a thin coating of ZnO nanorods which do not offer sufficient surface area for sensing applications. Therefore, 1 mM concentration was not investigated further. For 3 mM and 5 mM concentrations, strong and almost comparable optical absorption spectra for the ZnO nanorods were obtained. At higher growth cycles, the spectra in the visible region were found to increase, as shown in Figure 4.4, due to the visible light scattering from the longer ZnO nanorods formed at higher growth cycles. The values

marked in blue arrow in figure 4.4 indicates the samples which were further considered to deposit AuNPs. These samples showed comparable UV absorption characteristics from the ZnO nanorods with relatively small light scattering in the visible region.

Figure 4.4

Optical Absorption of ZnO Nanorods at 525 nm

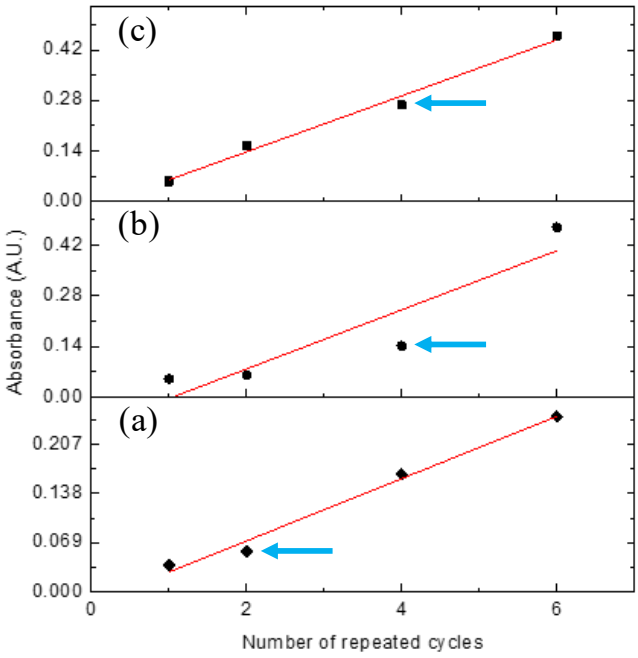

Note. The comparison of light absorption at specific wavelength (525 nm) of ZnO nanorods made from 1mM (a), 3mM (b), and 5mM (c) of growth solutions. The 525 nm wavelength was selected since AuNPs typically shows strong SPR absorption at this wavelength.

4.2 Au Nanoparticles Deposition on ZnO nanorods

4.2.1 Morphology of AuNPs

AuNPs were deposited on the selected ZnO nanorods samples using a photoreduction process as described in the previous chapter. In order to vary the amount of AuNPs, the deposition cycle was varied from 2 to 6. Samples were then characterized using SEM to investigate the morphological changes of the AuNPs as the number of deposition cycles was varied. Figure 4.5 shows the SEM micrographs of the AuNPs decorated ZnO nanorods at different AuNPs deposition cycles.

Figure 4.5

SEM Micrographs of AuNPs Deposited ZnO Nanorods Synthesized at Different Conditions.

	3mM ZnO nanorods	5mM ZnO nanorods
2-cycle Au deposition	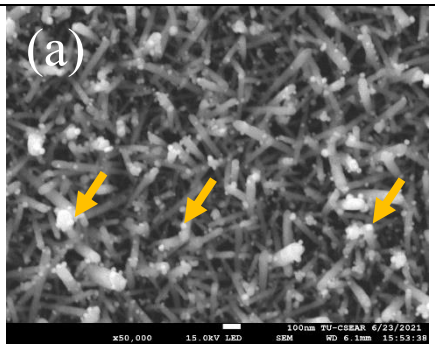	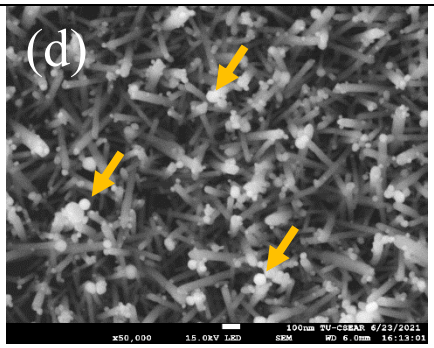
4-cycle Au deposition	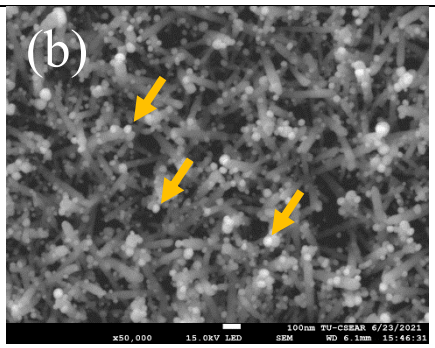	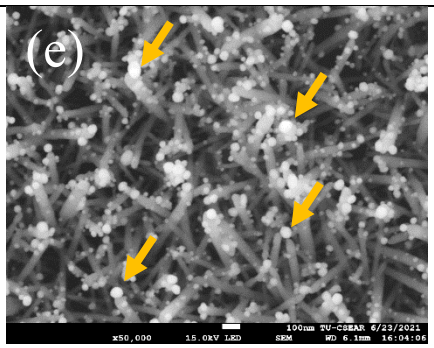
6-cycle Au deposition	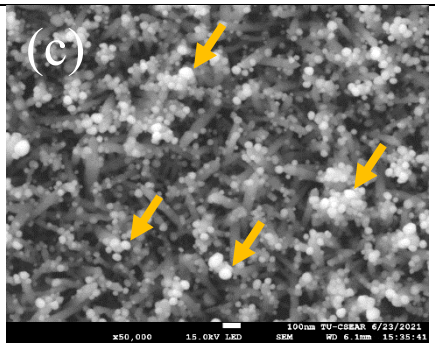	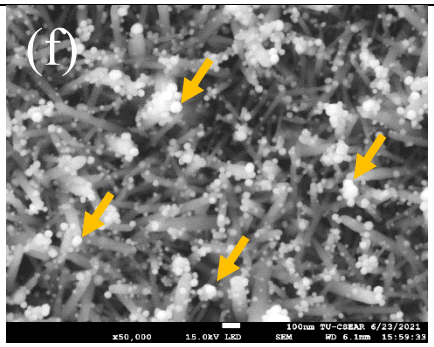

In all cases we observed almost spherical AuNPs deposited on the ZnO nanorods surface. The amount of AuNPs on both the ZnO nanorods samples (3 mM and 5 mM, respectively) was observed to increase as the number of AuNPs deposition cycles was increased from 2 to 6. At 6 deposition cycles, there was slight agglomeration of AuNPs

was observed with the appearance of slightly larger particle, but particles were found to maintain their spherical shape.

Figure 4.6

Average Diameter of AuNPs on ZnO Nanorods.

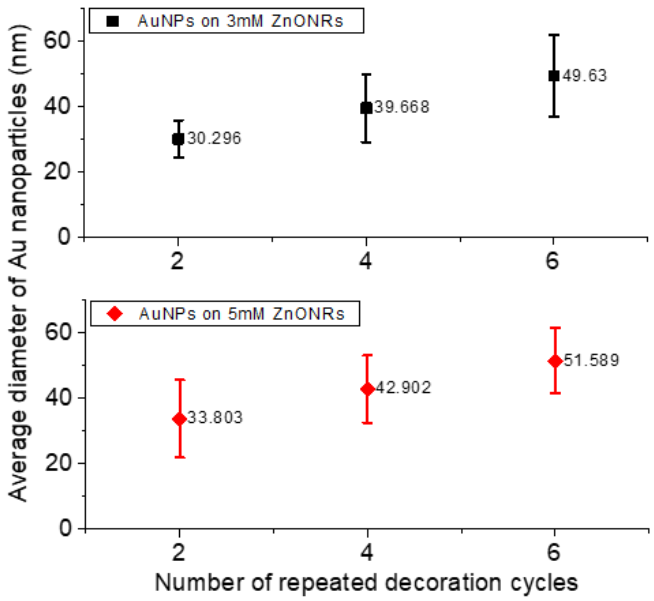

The average AuNPs size at deposition cycles 2, 4 and 6 were then estimated using ImageJ software, as shown in Figure 4.6. For the two ZnO nanorods samples almost comparable size of AuNPs were observed when deposition cycles were varied between 2 to 6. With the 3 mM ZnO nanorods samples the average diameter of the AuNPs was found to be around 30 nm at 2-deposition cycles, and it was almost linearly increased to about 50 nm at 6-deposition cycles. Similarly, for the 5 mM ZnO nanorods, the average AuNPs size was found to increase linearly from about 34 nm to 52 nm when the gold deposition cycles were varied from 2 to 6 respectively.

4.2.2 Elemental Analysis of the AuNPs Deposited ZnONRs

In order to estimate the amounts of gold deposition as the deposition cycles were varied, we carried our EDS elemental analysis of the samples. Figure 4.7 shows the atomic % ratio of the gold compared to the zinc collected from the EDS elemental analysis. For the 3 mM ZnO nanorods, the atomic % ratio of Au/Zn was observed to increase gradually from about 0.05 to about 0.15 as the gold deposition cycles were varied from 2 to 6, respectively, indicating higher amount of AuNPs deposition on the ZnO

nanorods at higher deposition cycles. The 5 mM ZnO nanorods samples however showed a slight drop in the atomic % ratio of Au/Zn at 6 deposition cycles compared to the 4-cycles. This is probably due to the etching of ZnO nanorods in the acidic gold chloride solution when exposed for longer period of times resulting in less AuNPs deposition. Overall, the 5 mM ZnO nanorod sample showed less atomic % ratio of Au/Zn due to the presence of higher amounts of ZnO compared to the 3 mM sample.

Figure 4.7

Atomic % Ratio of Au to Zn Estimated from EDS Elemental Analysis for Different AuNPs Deposited ZnO Nanorods.

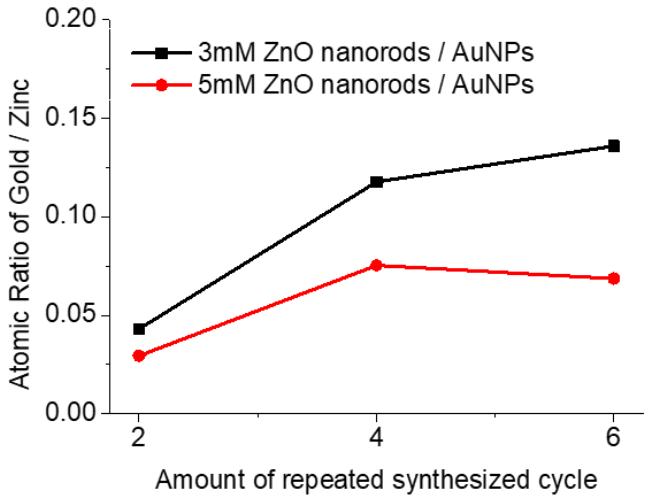

4.2.3 Optical Absorption of AuNPs Deposited ZnONRs

The optical absorption spectra of the AuNPs decorated ZnO nanorods were recorded using a UV-Visible spectrophotometer. Figure 4.8 shows the typical optical absorption spectra of AuNPs decorated ZnO nanorods synthesized at different concentrations. Form the figure it can be seen that all the samples showed the characteristic UV absorption band from ZnO nanorods as observed earlier, along with an addition visible light absorption band peaking at around 520 nm representing the LSPR absorption band due to the presence of the AuNPs in the sample. Both 3 and 5 mM ZnO samples showed comparable LSPR absorption indicating almost equal amounts and similar sizes of AuNPs on the samples. The 1 mM sample was shown for comparison where the LSPR absorption peak was hardly visible due to the very less amounts of ZnO deposition at 1 mM growth conditions. The 1 mM sample was used only for comparison purpose, and

no sensor was fabricated with this sample due to the very low optical signal from the sample.

Figure 4.8

UV-Visible Optical Absorption of AuNPs Decorated ZnO Nanorods.

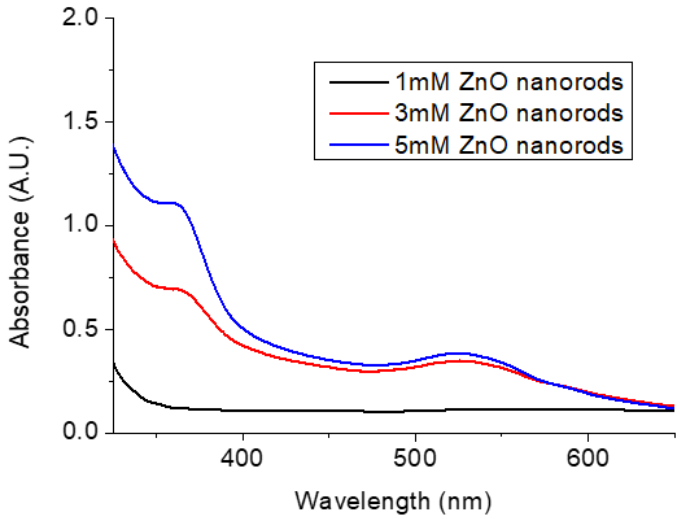

Note. Three different ZnO nanorods were used here grown at three different growth solution concentrations (1 mM, 3 mM, and 5 mM).

Figure 4.9

LSPR Absorption Peak Intensities of AuNPs on ZnONRs at 520 nm as a Function of the Number of Deposition Cycles.

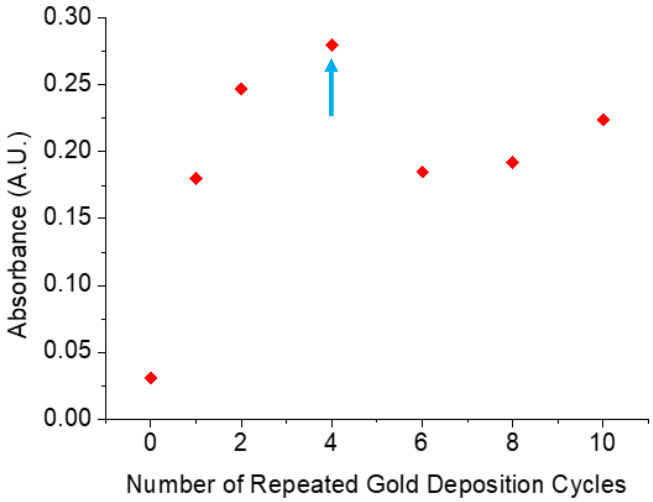

Figure 4.9 shows the intensity of the LSPR absorption peak at 520 nm as a function of AuNPs deposition cycles. With increasing deposition cycles from 2 to 4, the intensity of the LSPR absorption peak from the samples was observed to increase reaching a maximum value at 4 deposition cycles. After 4-cycles, a sudden drop in the LSPR absorption intensity was observed. This is probably due to the etching of ZnO nanorods when exposed to the acidic gold chloride solution for longer time resulting in desorption of AuNPs from the surface.

This also confirms the observations made during the EDS elemental analysis when the atomic % ration of Au/Zn was found maximum at 4-cycles and dropped slightly after that. However, the optical absorption of the 4 and 6 cycle samples, as shown in Figure 4.10, was found to be comparable and the 6-cycle sample showed slightly higher absorption intensity compared to the 4-cycle sample. Therefore, for our further studies, we considered both 4 and 6 cycle samples to construct the aptasensors. For comparison, we have shown the UV-visible spectra from all samples prepared with different number of ZnO nanorods synthesis cycles but the gold deposition cycle was fixed at 6 cycles in Figure 4.11.

Figure 4.10

The Optical Absorption of the AuNPs Decorated ZnONRs Prepared at Different Gold Deposition Cycles.

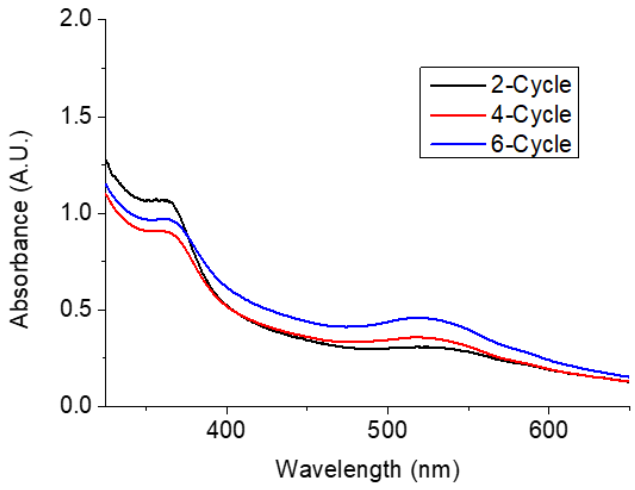

Figure 4.11

UV-Visible Absorption Spectra of AuNPs decorated ZnO Nanorods Obtained at Different Conditions of ZnO Nanorods Growth and AuNPs Deposition.

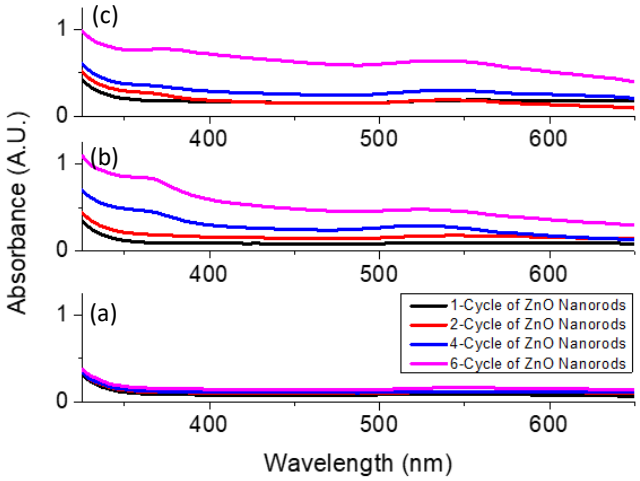

4.3 AuNPs Surface Functionalization with AMP17 Aptamer

To construct the aptasensor and improve its selectivity towards ampicillin, AMP17 aptamer was used to functionalize the AuNPs surface. After the surface modification was finished, the optical absorption was measured and compared with the absorption spectrum of the same sample recorded prior to the surface functionalization with AMP17 aptamer. There were 30 samples prepared for each ZnO nanorods growth conditions (3 mM and 5 mM growth solution concentrations) and decorated with AuNPs using 6 gold deposition cycles. After the AMP17 functionalization, all samples showed red-shift in their LSPR signals. Figure 4.12 shows the LSPR peak shifts of all the samples estimated from their respective UV-Visible absorption spectra. For 3 mM ZnO nanorods, an average red-shift of 19 nm was observed, while the 5 mM ZnO nanorod samples showed an average 11 nm of red-shifts. Visually also the samples showed a color change from dark magenta to violet, as shown in Figure 4.13, supporting the red-shift of the LSPR peak observed in the UV-Visible spectrophotometer. The red-shift of the LSPR peak therefore confirmed the successful surface functionalization of the AuNPs with the AMP17 aptamer molecules.

Figure 4.12

LSPR Peak Shift of the AuNPs After AMP17 Functionalization.

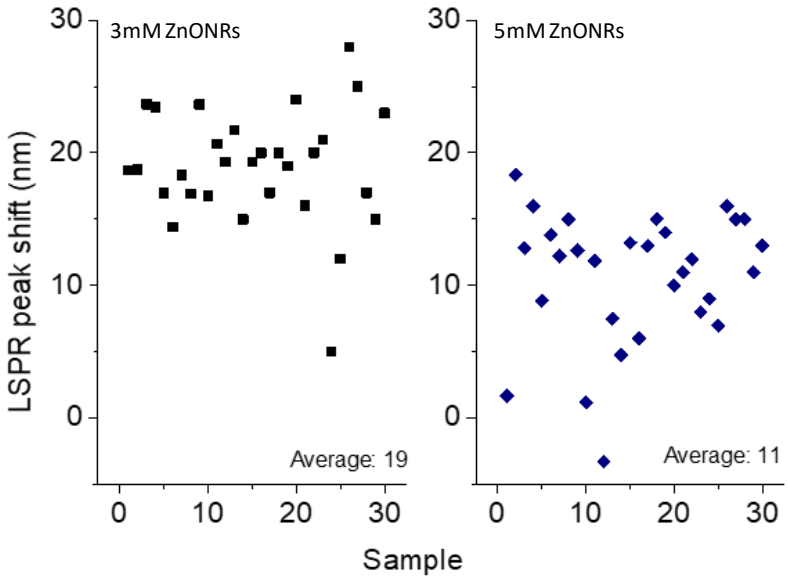

Note. Two ZnO nanorods samples were used where the nanorods were hydrothermally grown by using 3mM and 5 mM growth solution concentrations. AuNPs were deposited by using 6 deposition cycles.

Figure 4.13

The Change in Color of the AuNPs Decorated ZnO Nanorods Samples After AMP17 Aptamer Functionalization.

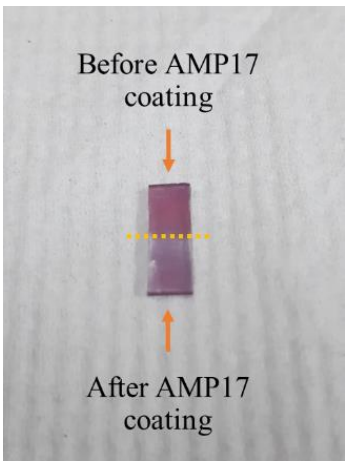

4.4 Ampicillin Sensor Fabrication and Performance Evaluation

After the surface functionalization of the AuNPs surface with the AMP17 aptamers, the construction of the aptasensor was complete and we started evaluating the sensor performance by exposing the aptasensor to ampicillin aqueous solution. Upon exposure to different concentrations of ampicillin the LSPR-based aptasensor produced further red-shift of the LSPR signal indicating binding of the ampicillin molecules to the AMP17 aptamers. The red-shift of the LSPR peak was used for detection and performance evaluation of the sensor. The assessment of the sensitivity of the fabricated LSPR-based aptasensor was done by testing the sensor with aqueous solution containing different concentrations of ampicillin ranging from 0 to 10 mg/L. The average LSPR peak shifts of the LSPR-based aptasensor before and after ampicillin measurement with different concentrations were collected from their respective optical absorption spectra. At least 3 replicas were used for each concentration of ampicillin to find out the average LSPR peak shift. Then, the recorded data was plotted against ampicillin concentrations, which is represented in Figure 4.14.

Figure 4.14

LSPR Peak Shift of the Aptamer Against Various Concentrations of Ampicillin

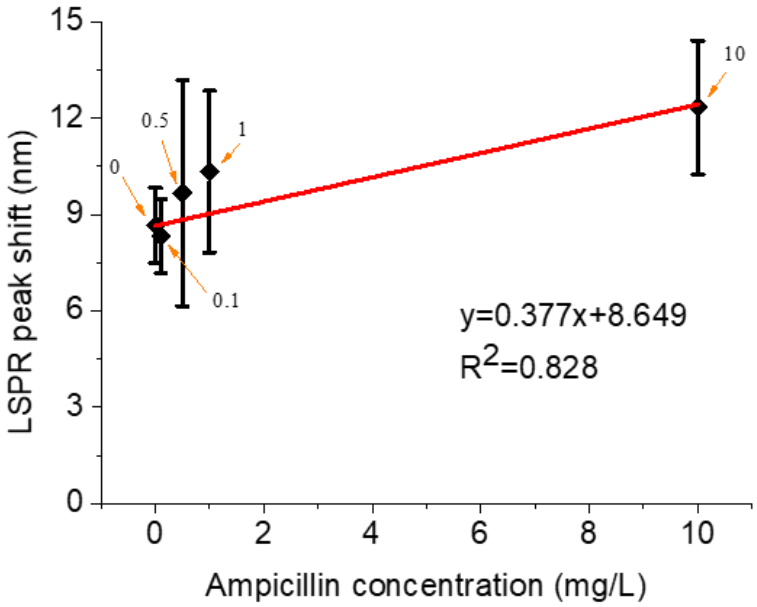

Using curve fitting in Figure 4.14, a linear regression curve was plotted to see the response of the sensor against different concentrations of ampicillin. The correlation

coefficient (R^2 value) of 0.828 was obtained for the linear regression which indicates that the sensor response has relatively large differences among the repeated measurements. From the slope of the linear regression curve the sensitivity of the sensor was estimated to be 0.38 nm per mg/L of ampicillin. The LOD of the aptasensor was then estimated by using equation 3.1 and found to be around 10.11 mg/L or approximately 10 mg/L (10 ppm).

4.5 Fabrication Protocol of LSPR-Aptasensor for Ampicillin Waste Detection in Water

Based on the results obtained and discussed in the previous sections, the following fabrication protocol for the LSPR-based aptasensor is proposed:

I. Prepare glass slides by cutting and cleaning them neatly to use as substrate for the sensing surface.
II. Spray 1 mM zinc acetate in ethanol solution on the glass substrate heated at ~80 °C, followed by annealing at 250 °C for five hours to obtain a ZnO seed layer.
III. Grow ZnO nanorods on the seeded glass substrates using hydrothermal process. Use 5mM zinc nitrate and hexamine aqueous solution to grow the ZnO nanorods with four repeated cycles of 30 minutes synthesis duration each. Anneal the ZnO nanorods at 350 °C for 1 hour.
IV. Deposit Au nanoparticles on the ZnO nanorods by photoreduction technique using 0.2 mM gold chloride solution. Expose the ZnO nanorods with UV light while immerged in the gold chloride solution for 5 minutes. Retract the sample, rinse with DI water, dry at 150 °C for 30 minutes and repeat the same process for a total of 6 times. Finally anneal the samples at 450 °C for 1 hour. Record the optical absorption spectrum of the substrate.
V. The fabricated AuNPs surface is functionalized by placing in 1 µM AMP17 solution (pH 8.0 ± 0.1) for 30 minutes then cleaned with TE buffer and dry in room temperature. Record the optical absorption spectrum of the substrate.
VI. The fabricated aptasensor is incubated in ampicillin aqueous solution for 10 minutes and dried at the room temperature. Record the optical absorption spectrum of the aptasensor substrate and estimate the LSPR peak shift.

VII. Calculate the sensitivity by plotting the LSPR peak shift against different concentrations of ampicillin and determine LOD

CHAPTER 5
CONCLUSION AND RECOMMENDATIONS

5.1 Conclusions

LSPR-based aptasensor composed of ZnO nanorods decorated with Au nanoparticles were successfully fabricated. The hydrothermal and photoreduction methods were utilized to create the LSPR sensor surface. The UV-visible optical absorption of the LSPR sensor surface clearly showed a UV absorption peak attributed to the ZnO nanorods and a visible light absorption band peaking at around 520 nm attributed to the LSPR peak of the AuNPs. Hydrothermally grown ZnO nanorods showed increase in the UV absorption intensity when higher growth solution concentrations and longer growth time was used and offered a very low optical absorption in the visible region. Similarly, the AuNPs produced stronger LSPR signal when their numbers were increased by multiple deposition cycles. The morphological characterization carried by the FE-SEM technique on the fabricated ZnO nanorods indicated the characteristic hexagonal shape of the nanorods with average diameter up to 70 nm. AuNPs decorated on the synthesized ZnO nanorods exhibited a round shape with average sizes varied between 30 to 50 nm. The best condition to fabricate the LSPR sensor with less signal interference between ZnO and Au and strong LSPR signal was found when ZnO nanorods were grown using 5 mM growth solution concentrations with 4 repeated growth cycles (where each cycle time is 1 hour), and AuNPs were deposited with 6 photoreduction cycles.

The LSPR-based aptasensor was fabricated by functionalizing the AuNPs surface using AMP17 aptamer specific to ampicillin. The fabricated aptasensor showed a red-shift in the LSPR absorption spectrum once exposed to the ampicillin solution in water, which was continuously increased with increasing ampicillin concentrations varied between 0.1 to 10 mg/L. The sensitivity estimated for the aptasensor was found to be around 0.38 nm per mg/L ampicillin in water with a LOD value around 10 mg/L. The results obtained in this study therefore demonstrates the potential use of LSPR-based aptasensors for ampicillin detection in water which can be fabricated using inexpensive techniques, and its simple and smaller size make it suitable for real-time and mobile

detection applications. Nevertheless, further sensor element design modification is necessary to lower the detection limit of the LSPR-based aptasensor.

5.2 Recommendations

Based on the results obtained in this study following recommendations are made for future research:

1) In order to improve the reproducibility of the aptasensor, further investigated is necessary for controlled growth of ZnO nanorods. This can be achieved by carefully controlling the various parameters of the hydrothermal growth technique used for ZnO nanorods, such as pH, temperature, slow growth conditions and concentration of the growth solution. In addition, other deposition methods for ZnO, such as electrodeposition, chemical vapor deposition or template assisted growth can be explored to obtain a uniform ZnO coating.

2) Further investigations on deposition methods to obtain uniform size of Au nanoparticles should be carried out to ensure stable LSPR signal.

3) More detailed investigation on the aptamer functionalization on the AuNPs surface is necessary to ensure uniformity of the sensor surface and improved reproducibility of the sensor performance.

4) Alternatives of aptamers, such as antibodies can be explored further to improve the sensitivity of the LSPR sensor for pharmaceutical waste detection.

REFERENCES

Bacanlı, M., & Başaran, N. (2019a). Importance of antibiotic residues in animal food. *Food and Chemical Toxicology*, *125*(October 2018), 462–466. https://doi.org/10.1016/j.fct.2019.01.033

Bacanlı, M., & Başaran, N. (2019b). Importance of antibiotic residues in animal food. *Food and Chemical Toxicology*, *125*(January), 462–466. https://doi.org/10.1016/j.fct.2019.01.033

Bound, J. P., & Voulvoulis, N. (2005). Household disposal of pharmaceuticals as a pathway for aquatic contamination in the United Kingdom. *Environmental Health Perspectives*, *113*(12), 1705–1711. https://doi.org/10.1289/ehp.8315

Bueno, M. J. M., Gomez, M. J., Herrera, S., Hernando, M. D., Agüera, A., & Fernández-Alba, A. R. (2012). Occurrence and persistence of organic emerging contaminants and priority pollutants in five sewage treatment plants of Spain: Two years pilot survey monitoring. *Environmental Pollution*, *164*, 267–273. https://doi.org/10.1016/j.envpol.2012.01.038

Cao, J., Galbraith, E. K., Sun, T., & Grattan, K. T. V. (2011). Comparison of surface plasmon resonance and localized surface plasmon resonance-based optical fibre sensors. *Journal of Physics: Conference Series*, *307*(1). https://doi.org/10.1088/1742-6596/307/1/012050

Cho, E. J., Lee, J.-W., & Ellington, A. D. (2009). Applications of Aptamers as Sensors. *Annual Review of Analytical Chemistry*, *2*(1), 241–264. https://doi.org/10.1146/annurev.anchem.1.031207.112851

Feng, B., Zhu, R., Xu, S., Chen, Y., & Di, J. (2018). A sensitive LSPR sensor based on glutathione-functionalized gold nanoparticles on a substrate for the detection of Pb2+ ions. *RSC Advances*, *8*(8), 4049–4056. https://doi.org/10.1039/c7ra13127e

Franco, D. A., Webb, J., & Taylor, C. E. (1990). Antibiotic and sulfonamide residues in meat: Implications for human health. *Journal of Food Protection*, *53*(2), 178–185. https://doi.org/10.4315/0362-028X-53.2.178

Gai, P., Gu, C., Hou, T., & Li, F. (2017). Ultrasensitive Self-Powered Aptasensor Based on Enzyme Biofuel Cell and DNA Bioconjugate: A Facile and Powerful Tool for Antibiotic Residue Detection. *Analytical Chemistry*, *89*(3), 2163–2169. https://doi.org/10.1021/acs.analchem.6b05109

Gelband, H., Miller-Petrie, M., Pant, S., Gandra, S., Levinson, J., Barter, D., White, A., & Laxminarayan, R. (2015). The state of the world's antibiotics 2015. *Wound Healing Southern Africa*, *8*(2), 30–34. https://journals.co.za/content/mp_whsa/8/2/EJC180082

Hammesfahr, U., Bierl, R., & Thiele-Bruhn, S. (2011). Combined effects of the antibiotic sulfadiazine and liquid manure on the soil microbial-community structure and functions. *Journal of Plant Nutrition and Soil Science*, *174*(4), 614–623. https://doi.org/10.1002/jpln.201000322

Homola, J. (2008). Surface plasmon resonance sensors for detection of chemical and biological species. *Chemical Reviews*, *108*(2), 462–493. https://doi.org/10.1021/cr068107d

Hou, L., Yin, G., Liu, M., Zhou, J., Zheng, Y., Gao, J., Zong, H., Yang, Y., Gao, L., & Tong, C. (2015). Effects of sulfamethazine on denitrification and the associated N2O release in estuarine and coastal sediments. *Environmental Science and Technology*, *49*(1), 326–333. https://doi.org/10.1021/es504433r

Huang, C.-H., Renew, J. E., Smeby, K. L., Pinkston, K., & Sedlak, D. L. (2001). Assessment of Potential Antibiotic Contaminants in. *Journal of Contemporary Water Research and Education*, *120*(1), 30–40.

Kadam, A., Patil, S., Patil, S., & Tumkur, A. (2016). Pharmaceutical Waste Management An Overview. *Indian Journal of Pharmacy Practice*, *9*(1), 2–8. https://doi.org/10.5530/ijopp.9.1.2

Lapworth, D. J., Baran, N., Stuart, M. E., & Ward, R. S. (2012). Emerging organic contaminants in groundwater: A review of sources, fate and occurrence. *Environmental Pollution*, *163*, 287–303. https://doi.org/10.1016/j.envpol.2011.12.034

Lee, M.H., Lee, H.J., Ryu, P. D. (2001). Lee et al 2001 Chemical and antibiotic resides.pdf. In *Asian-Australian Journal of Animal Science* (Vol. 14, Issue 3, pp. 402–413).

Li, F., Guo, Y., Wang, X., & Sun, X. (2018a). Multiplexed aptasensor based on metal ions labels for simultaneous detection of multiple antibiotic residues in milk. *Biosensors and Bioelectronics*, *115*(59), 7–13. https://doi.org/10.1016/j.bios.2018.04.024

Li, F., Guo, Y., Wang, X., & Sun, X. (2018b). Multiplexed aptasensor based on metal ions labels for simultaneous detection of multiple antibiotic residues in milk.

Biosensors and Bioelectronics, *115*, 7–13. https://doi.org/10.1016/j.bios.2018.04.024

Li, W. C. (2014). Occurrence, sources, and fate of pharmaceuticals in aquatic environment and soil. *Environmental Pollution*, *187*, 193–201. https://doi.org/10.1016/j.envpol.2014.01.015

Lim, Y. C., Kouzani, A. Z., & Duan, W. (2010). Aptasensors: A review. *Journal of Biomedical Nanotechnology*, *6*(2), 93–105. https://doi.org/10.1166/jbn.2010.1103

Lin, Y., Zhao, M., Guo, Y., Ma, X., Luo, F., Guo, L., Qiu, B., Chen, G., & Lin, Z. (2016). Multicolor colormetric biosensor for the determination of glucose based on the etching of gold nanorods. *Scientific Reports*, *6*(November), 1–7. https://doi.org/10.1038/srep37879

Luo, Z., Wang, Y., Lu, X., Chen, J., Wei, F., Huang, Z., Zhou, C., & Duan, Y. (2017). Fluorescent aptasensor for antibiotic detection using magnetic bead composites coated with gold nanoparticles and a nicking enzyme. *Analytica Chimica Acta*, *984*, 177–184. https://doi.org/10.1016/j.aca.2017.06.037

Marshall, B. M., & Levy, S. B. (2011). Food animals and antimicrobials: Impacts on human health. *Clinical Microbiology Reviews*, *24*(4), 718–733. https://doi.org/10.1128/CMR.00002-11

Masson, J. F. (2020). Portable and field-deployed surface plasmon resonance and plasmonic sensors. *Analyst*, *145*(11), 3776–3800. https://doi.org/10.1039/d0an00316f

Microfluidic, F. O. F. (n.d.). *Design and Fabrication of Microfluidic Devices : May 2020*, 321–327.

Murray, K. E., Thomas, S. M., & Bodour, A. A. (2010). Prioritizing research for trace pollutants and emerging contaminants in the freshwater environment. *Environmental Pollution*, *158*(12), 3462–3471. https://doi.org/10.1016/j.envpol.2010.08.009

O'Sullivan, C. K. (2002). Aptasensors - The future of biosensing? *Fresenius' Journal of Analytical Chemistry*, *372*(1), 44–48. https://doi.org/10.1007/s00216-001-1189-3

Petryayeva, E., & Krull, U. J. (2011). Localized surface plasmon resonance: Nanostructures, bioassays and biosensing-A review. *Analytica Chimica Acta*, *706*(1), 8–24. https://doi.org/10.1016/j.aca.2011.08.020

Rafailidis, P. I., Ioannidou, E. N., & Falagas, M. E. (2007). Ampicillin/sulbactam:

Current status in severe bacterial infections. *Drugs*, *67*(13), 1829–1849. https://doi.org/10.2165/00003495-200767130-00003

Rostami, S., Mehdinia, A., Niroumand, R., & Jabbari, A. (2020). Enhanced LSPR performance of graphene nanoribbons-silver nanoparticles hybrid as a colorimetric sensor for sequential detection of dopamine and glutathione. *Analytica Chimica Acta*, *1120*, 11–23. https://doi.org/10.1016/j.aca.2020.04.060

Shrivas, K., Sahu, J., Maji, P., & Sinha, D. (2017). Label-free selective detection of ampicillin drug in human urine samples using silver nanoparticles as a colorimetric sensing probe. *New Journal of Chemistry*, *41*(14), 6685–6692. https://doi.org/10.1039/c7nj00448f

Shrivastava, A., & Gupta, V. (2011). Methods for the determination of limit of detection and limit of quantitation of the analytical methods. *Chronicles of Young Scientists*, *2*(1), 21. https://doi.org/10.4103/2229-5186.79345

Smith, W. E. (2007). Surface Enhanced Resonance Raman Scattering. *Pharmaceutical Applications of Raman Spectroscopy*, 65–84. https://doi.org/10.1002/9780470225882.ch3

Sönnichsen, C. (2001). Plasmons in metal nanostructures. *Dissertation*, *27*(June), 134. http://edoc.ub.uni-muenchen.de/2367/1/Soennichsen_Carsten.pdf

SPRtech101. (2011, September 30). Surface Plasmon Resonance Explained [Video]. https://youtu.be/sM-VI3alvAI

Srivastava, A. K., Yadev, R., Rai, V. N., Ganguly, T., & Deb, S. K. (2012). Surface plasmon resonance in gold nanoparticles. *AIP Conference Proceedings*, *1447*(1), 305–306. https://doi.org/10.1063/1.4710001

Suksrimuang, T. (2006). *การวิเคราะห์สมบัติทางเคมีไฟฟ้าโดยวิธีไซคลิกโวลแทมเมตทรี* [Electrochemical analysis by cyclic voltammetry method]. Pathumthani, Thailand: MTEC.

The Audiopedia. (2018, February 6). What is LOCALIZED SURFACE PLASMON? What does LOCALIZED SURFACE PLASMON mean? [Video]. https://youtu.be/vtR3RYgS9Eo

Thi, L., & Hiep, T. (n.d.). *DESIGN AND FABRICATION OF MICROFLUIDIC LSPR*. *May 2020*.

Tombelli, S., Minunni, M., & Mascini, M. (2005). Analytical applications of aptamers. *Biosensors and Bioelectronics*, *20*(12), 2424–2434. https://doi.org/10.1016/j.bios.2004.11.006

Vieno, N. M., Härkki, H., Tuhkanen, T., & Kronberg, L. (2007). Occurrence of pharmaceuticals in river water and their elimination in a pilot-scale drinking water treatment plant. *Environmental Science and Technology*, *41*(14), 5077–5084. https://doi.org/10.1021/es062720x

Wang, X., Dong, S., Gai, P., Duan, R., & Li, F. (2016). Highly sensitive homogeneous electrochemical aptasensor for antibiotic residues detection based on dual recycling amplification strategy. *Biosensors and Bioelectronics*, *82*, 49–54. https://doi.org/10.1016/j.bios.2016.03.055

VITA

Born in 1996, Khajohnpat Teerasitwaratorn earned his B.Sc. degree in Applied Physics from the King Mongkut's University of Technology North Bangkok, Thailand in 2019. During his bachelor's degree he worked as a research intern at the Carbon-based Devices and Nanoelectronics Laboratory (CNL) in National Electronics and Computer Technology Center (NECTEC), Thailand. Right after his bachelor's degree, he joined Asian Institute of Technology to pursue his master's degree in Nanotechnology field. During his master's degree, Khajohnpat has received financial assistance in the form of the Royal Thai Government Fellowship. His broad research interest is in the synthesis of nanomaterials and their applications in the field of sensing. He is currently exploring the area of self-healing materials for sensor design to continue his research career.